




# Phosphorous-based epoxy resin composition as an effective anticorrosive coating for steel

O. Dagdag<sup>1</sup> · A. El Harfi<sup>1</sup> · A. Essamri<sup>1</sup> · M. El Gouri<sup>1,2</sup> · S. Chraïbi<sup>3</sup> · M. Assouag<sup>3</sup> · B. Benzidia<sup>4</sup> · O. Hamed<sup>5</sup> · H. Lgaz<sup>6</sup> · S. Jodeh<sup>5</sup> 

Received: 25 March 2017 / Accepted: 11 September 2018 / Published online: 20 September 2018  
© The Author(s) 2018

## Abstract

Epoxy resin (ER) is an attractive material for metal protection against corrosion; it can form a strongly adhered film onto a metal surface through its multi coordination sites. In this study, an epoxy resin-based formulation was designed, prepared, and applied onto steel surface with and without a pigment. The anticorrosive formulation (ER–MDA–ZP) was prepared from the ER and the hardener 4,4'-methylene dianiline (MDA) in the presence of the anticorrosive pigment zinc phosphate (ZP). A second standard formulation (ER–MDA) was prepared without ZP. The epoxy and the hardener react to form a 3D cross-linked polymeric network with multicoordination sites (hydroxyl and amino groups) for metals. The characterization of the epoxy resin was performed using Fourier transform infrared spectroscopy (FTIR) and nuclear magnetic resonance (<sup>1</sup>H and <sup>31</sup>P NMR). Both samples exhibited excellent thermal properties as they subjected to thermal analysis using differential scanning calorimetry. The ER–MDA–ZP formulation showed a higher glass transition temperature ( $T_g$ ) than ER–MDA. The coated steel specimens were immersed for 1 h in a 3 wt% NaCl solution and their anticorrosive properties were monitored by electrochemical impedance spectroscopy (EIS). The total resistance ( $R_t$ ) values obtained by the EIS method for the ER–MDA and ER–MDA–ZP formulations were 21,383  $\Omega$  cm<sup>2</sup> and 55,143  $\Omega$  cm<sup>2</sup>, respectively. The coated steel samples after the acid treatment were subjected to aging by exposing them to a UV light for 2000 h. The aging caused the  $R_t$  values to drop to 1621  $\Omega$  cm<sup>2</sup> and 7264  $\Omega$  cm<sup>2</sup>, respectively. The results indicate the formation of a highly stable film of ER–MDA–ZP formulation on the steel surface that withstands an accelerated corrosive environment of 2000 h exposure to UV light and 1 h of immersion in a 3 wt% NaCl.

**Keywords** Epoxy coatings · Zinc phosphate · Carbon steel · 3 wt% NaCl · Ultraviolet radiation · Electrochemical impedance spectroscopy

✉ S. Jodeh  
sjodeh@hotmail.com

<sup>1</sup> Laboratory of Agroresources, Polymers and Process Engineering, Team of Macromolecular and Organic Chemistry, Department of Chemistry, Faculty of Science, Ibn Tofail University, BP 133, 14000 Kenitra, Morocco

<sup>2</sup> Laboratory of Process, Renewable Energy and Environment, Department of Process Engineering, Height School of Technology, Sidi Mohammed Ben Abdallah University, Fez, Morocco

<sup>3</sup> Team of Materials, Metallurgy and Process Engineering, ENSAM, University Moulay Ismail, B.P. 15290, Al Mansour, Meknes, Morocco

<sup>4</sup> Laboratory of Materials, Electrochemistry and Environment, Department of Chemistry, Faculty of Sciences, Ibn Tofail University, Kenitra, Morocco

<sup>5</sup> Department of Chemistry, An-Najah National University, P. O. Box 7, Nablus, Palestine

<sup>6</sup> Department of Applied Bioscience, College of Life and Environment Science, Konkuk University, 120 11 Neungdong-ro, Gwangjin-gu, Seoul 05029, South Korea



## Introduction

Organic-based materials with metal adhesion properties are widely used as metal anticorrosive agents in many industries include aeronautics, automobiles, architecture, ships, and oil tanks [1]. They are usually applied on the metal surface as a thin film, thus preventing the corrosive agents from reaching the metal surface [2]. Epoxy resin-based materials are among the most widely organic-based materials, since they have unique properties and versatility [3]. Epoxy resins have outstanding thermal stability, tensile strength, and superior thermal adhesion, mechanical and anticorrosive characteristics in addition to their exceptional surface properties like low shrinkage, ease of cure and high moisture, solvent and chemical resistance, and excellent adhesion performance [4]. Unfortunately, most of the reported epoxy formulations are based on conventional diglycidyl ether of bisphenol-A (DGEBA) and novolac epoxy resins which are carcinogenic and toxic.

Anticorrosion pigments are usually included in epoxy formation to enhance its stability and performance, the most widely used pigment in the epoxy coatings chromate-based materials. However, due to environmental concerns, the use of the chromate-based pigments was very limited. Currently, there is a great interest in a new generation of anticorrosive pigments that are environmentally friendly and have high efficiency to replace the chromate-based pigments [5, 6]. Zinc phosphate was suggested as a replacement for zinc chromate. The toxicity of zinc phosphate is 50 times less than zinc chromates [7]. Pigments based on phosphates have been reported so far by several scientific groups and showed a high tendency to enhance the anticorrosion performance of the organic coating and its adhesion to steel substrate [8, 9].

The toxicity and possible carcinogenicity of the current formulation has motivated us to offer a new formulation based on new nontoxic epoxy resin for metal protection in the aggressive marine corrosive environment.

In this work, a new formulation that is a combination of epoxy resin hexaglycidyl tris (*p*-ethylene dianiline) phosphoric triamide (ER) and curing agent a 4,4'-methylene dianiline (MDA) containing the anticorrosive protective pigment zinc phosphate was developed. The combination of these three materials produced a steel coating that can endure aggressive marine environment where UV is very intense, and the humidity and salts are high [10].

The anticorrosion property of the formulation was monitored by the electrochemical impedance spectroscopy (EIS); the obtained data were used to assess the coating performance.

## Experimental

### Materials and methods

All reagents and solvents used in this work like 4,4'-ethylene dianiline (EDA), phosphorus oxychloride ( $\text{POCl}_3$ ), epichlorohydrin, triethylamine, ethanol, 4,4'-methylene dianiline (MDA), and zinc phosphate (ZP) were from Aldrich chemical company and used as they received.

Infrared (IR) spectra were registered on a Bruker Fourier transform infrared (FTIR) using the FTIR-attenuated total reflection technique. The following parameters were used: resolution  $4\text{ cm}^{-1}$ , spectral range  $400\text{--}4000\text{ cm}^{-1}$ , and number of scans 128.

The  $^1\text{H}$  and  $^{31}\text{P}$  NMR were recorded on a 300 MHz Bruker Avance spectrometer using deuterated dimethyl sulfoxide ( $\text{DMSO-d}_6$ ) as the solvent with tetramethylsilane (TMS) as a reference.

The calorimetric analysis was performed using a Shimadzu differential scanning calorimeter (DSC-60). The experiments were carried out under a constant flow of nitrogen using aluminum pans at a heating rate of  $20\text{ }^\circ\text{C min}^{-1}$  for a temperature range from 20 to  $300\text{ }^\circ\text{C}$ .

The composition of steel samples used in this study is given in Table 1, and the physical and chemical properties of the Zinc phosphate (ZP) are given in Table 2.

### Synthesis of hexaglycidyl tris (*p*-ethylene dianiline) phosphoric triamide (ER)

To a two-necked round bottom flask, fitted with a condenser, a magnet bar was added 10.0 g of 4,4'-ethylene dianiline ( $5 \times 10^{-2}\text{ mol}$ ) flowed by a dropwise addition of a 2.5 g of phosphorus trichloride. The resulting mixture

**Table 2** Physical and chemical properties of the zinc phosphate (ZP)

Composition	Zinc phosphate tetrahydrate $\text{Zn}_3(\text{PO}_4)_2(\text{H}_2\text{O})_4$
Commercial name	Zinc phosphate ZP
Density	$3.04\text{ g cm}^{-3}$
Average particle size	$4.5\text{ }\mu\text{m}$
Oil absorption	$27\text{ cm}^3/100\text{ g}$
pH	7
Solubility	Insoluble in water (water: $0.03\text{ g L}^{-1}$ )

**Table 1** Composition of the base metal carbon steel

C	Mn	Si	Al	Cr	Mo	Ni	Cu	Co	V	Fe
0.11	0.47	0.24	0.03	0.12	0.02	0.1	0.14	<0.001	<0.003	Balance

was stirred for 3 days at room temperature. Then, 9.0 g of epichlorohydrin was added at once. The reaction mixture temperature was raised to 80 °C and maintained at this temperature for 4 h. The reaction mixture was then cooled down to 40 °C and to it was added 10.0 g of triethylamine. The reaction was stirred for 3 h, and then, the solvent and the excess epichlorohydrin were removed under reduced pressure using a rotary evaporator. The residue was very viscous with a yellow color (73% yield).

### Epoxy resin-coating formulation

Two epoxy resin formulations ER–MDA and ER–MDA–ZP were prepared by mixing a stoichiometric amount of MDA hardener and epoxy resin (ER) without and with the zinc phosphate pigment. First, the zinc phosphate pigment was added to the epoxy resin (ER) at a concentration of 5 wt%. Then, a stoichiometric amount of MDA hardener was added to the mixture. Isopropyl alcohol was used as a diluent. A schematic diagram of the preparation epoxy formulation is shown in Fig. 1.

The two formulations were applied onto specimens of carbon steel by a film applicator. The surface of all steel specimens was sanded using sandpaper 600, 800, and 1200 grit, and then decreased with ethanol before coating. Coated steel samples were placed in 70 °C oven for 4 h under vacuum to complete curing and removal of the solvent. The thickness of dry coatings ( $170 \pm 10 \mu\text{m}$ ) was measured by a digital-coating thickness gage (Layercheck 750 USB FN). The thickness of the three specimens from each series was measured to check the reproducibility.

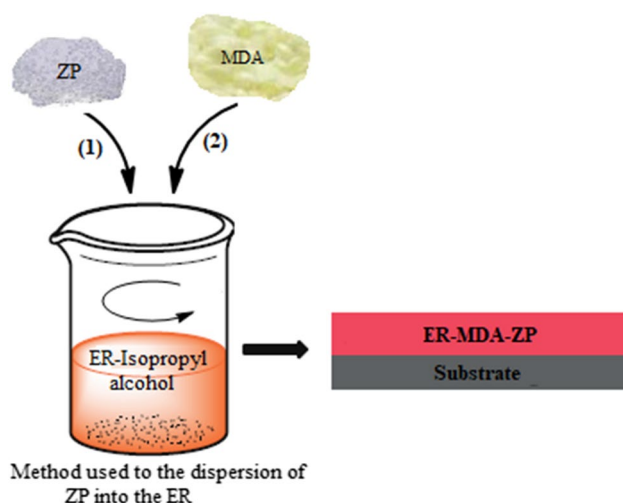


**Fig. 1** Schematic diagram shows the preparation of the epoxy resin formulation

### Coating evaluation under accelerated exposure conditions

The coating evaluation under accelerated exposure conditions was carried out by exposing the coated specimens to UV radiation. Commercial UV-A lamps (center wavelength of radiation 340 nm) were used for this purpose. The UV radiation with a power density of  $50 \text{ mW cm}^{-2}$  was applied. The aging temperature was regulated at 30 °C in the presence of oxygen (at room temperature range between 293 and 303 K). All samples were exposed to UV radiation for 2000 h with a geometric area of  $1 \text{ cm}^2$ .

### Electrochemical impedance spectroscopy analysis

Electrochemical impedance spectroscopy measurements were carried out using a Potentiostat PS 200. The measurements were carried out in a 3 wt% NaCl solution at room temperature. A three-electrode setup was used, consisting of a saturated calomel electrode (SCE), as a reference (RE), a Pt ring as the counter electrode (CE), and pieces cut from the coated carbon steel samples with a geometric area of  $1 \text{ cm}^2$  as the working electrode (WE).

All measurements were carried out at the open-circuit potential (OCP), using 10 mV amplitude of the sinusoidal voltage, over a frequency range of 100 kHz–10 MHz. The experimental data were analyzed and fitted with EC-Lab.

## Results and discussion

### Synthesis of the epoxy resin hexaglycidyl tris (*p*-ethylene dianiline) phosphoric triamide (ER)

Preparation of the epoxy resin hexaglycidyl tris (*p*-ethylene dianiline) phosphoric triamide (ER) was carried out as shown in Fig. 2. As shown in Fig. 2, 4,4'-ethylene dianiline was first reacted with phosphorus trichloride ( $\text{POCl}_3$ ) to produce phosphoric triamide. Treatment of phosphoric triamide with epichlorohydrin and then triethylamine produces the target product [11].

### Hardening of hexaglycidyl tris (*p*-ethylene dianiline) phosphoric triamide

The reaction of epoxy resin with the curing agent such as a polyamine compound is known as a hardening process. The hardening process usually initiated with heat and then become spontaneous and exothermic [12, 13]. The curing agent chosen for this work is 4,4'-methylene dianiline (MDA) (Fig. 3); it was chosen, because it has an aromatic moiety, which provides a very good thermal stability and good mechanical integrity to the resin [14].



**Fig. 2** Schematic diagram showing the total synthesis of ER

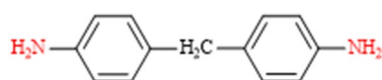
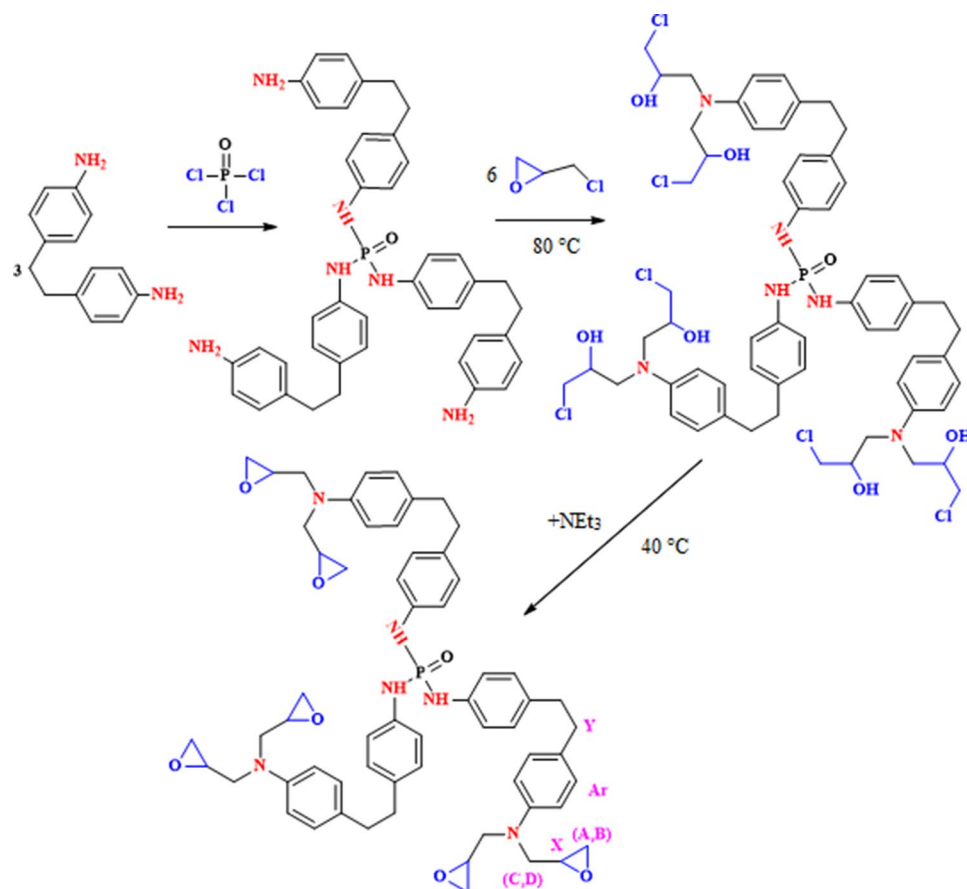


**Fig. 3** Chemical structure of 4,4'-methylene dianiline (MDA)

A representative scheme showing the reaction between the epoxide EP and the diamine MDA is shown in Fig. 4. As shown in Fig. 4, as the polymerization process is initiated by a nucleophilic attack of an amine on the epoxy ring, the propagation stage then follows, which leads to the formation of a three-dimensional polymer, as shown in Fig. 5 [15, 16].

Mixing of the epoxy resin with the hardener prior to crosslinking is performed differently depending on the hardening agent used. With the methylene dianiline (MDA), the protocol reported in the literature [16] is that methylene dianiline is placed in an oven at 120 °C (above its melting point), while the resin is heated to 60 °C. The two reagents while, in the liquid phase, are mixed and cured at 70 °C. In other reported process, an excess amount of epichlorohydrin was used as a reagent and solvent. Since it is a carcinogenic material, in this work, it was replaced with isopropyl alcohol as a solvent.

Zinc phosphate was also included in the coating to enhance the corrosion resistance [17].

## Epoxy resin and coating formulation analysis

### FTIR of ER and cured epoxy resin ER–MDA

The obtained ATR-FTIR spectrum of the phosphorus-containing epoxy resin is shown in Fig. 6. The spectrum shows several characteristics of bands. Two bands appear at 930  $\text{cm}^{-1}$  corresponding to the vibration of the oxirane ring [18]. Two bands also appear at 1060  $\text{cm}^{-1}$  and 1260  $\text{cm}^{-1}$  which correspond to the asymmetric vibrations of P–N group [19]. The two peaks at 1207  $\text{cm}^{-1}$  and 1020  $\text{cm}^{-1}$  are corresponding to (P=O) of phosphate compounds [20, 21]. A symmetric vibration band at 1191  $\text{cm}^{-1}$  could be attributed to the NP(O)N<sub>2</sub> group [18]. Other peaks at 1360  $\text{cm}^{-1}$ , 1450  $\text{cm}^{-1}$ , and 1510  $\text{cm}^{-1}$  are corresponding to the N–H vibration [22]. A broad peak appears at 3300  $\text{cm}^{-1}$  which could be related to residual OH. The band at 1611  $\text{cm}^{-1}$  could be attributed to C=C aromatic of the aromatic ring [23]. The multiple weak bands appear between 2840 and 2910  $\text{cm}^{-1}$  are characteristic bands of C–H vibrations [23].

**Fig. 4** Proposed mechanism for the reaction of an epoxy resin with the polyamine

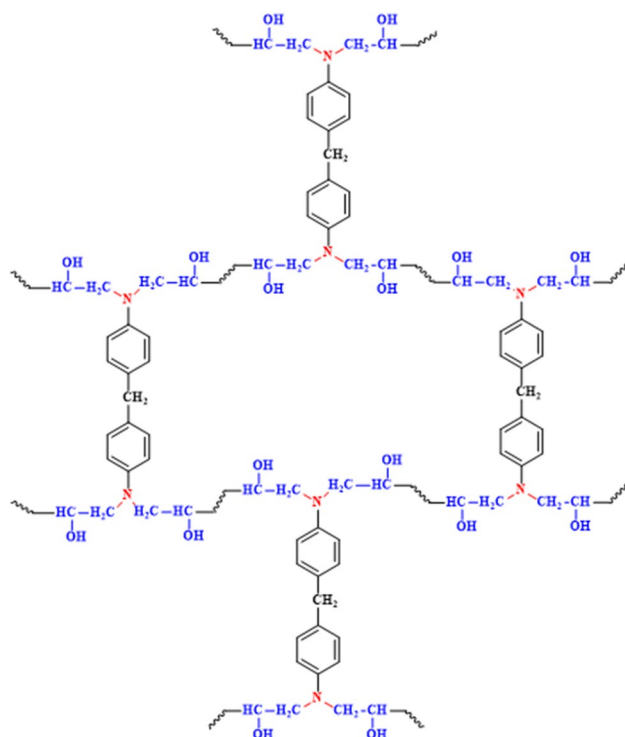
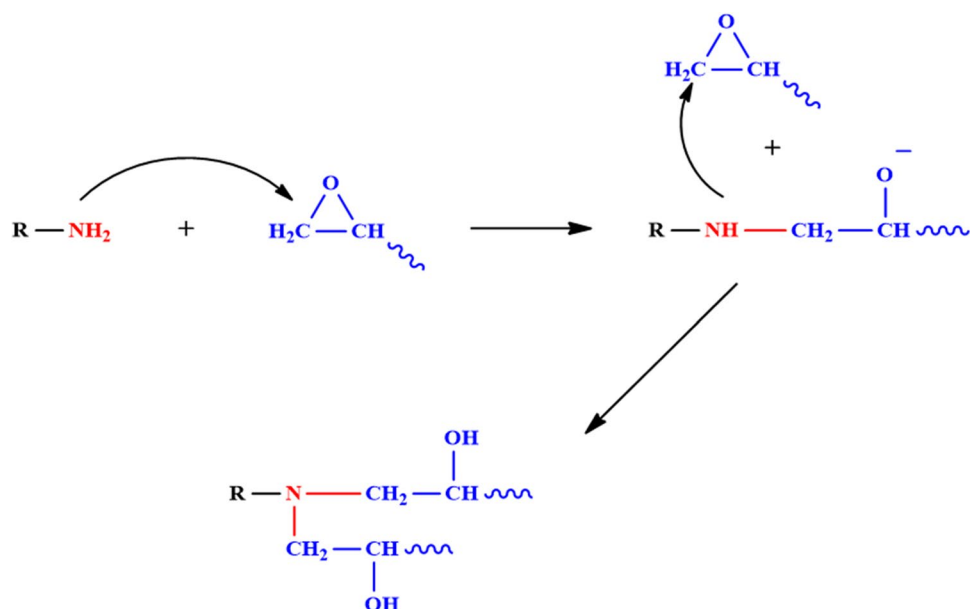


**Fig. 5** Possible chemical structure of epoxy resin polymeric network

The ATR-FTIR spectrum of hexaglycidyl tris (*p*-ethylene dianiline) phosphoric triamide cured with methylene dianiline on the steel surface is shown in Fig. 6. The characteristic absorption peaks shown in the spectrum are as follows:  $998\text{ cm}^{-1}$ ,  $1019\text{ cm}^{-1}$ , and  $1091\text{ cm}^{-1}$  corresponding to the asymmetric vibrations of P–N–C group;  $1184\text{ cm}^{-1}$  peak is corresponding to P=O stretching which is characteristic

of phosphate compounds; the peak at  $1226\text{ cm}^{-1}$  is corresponding to C–N vibrations;  $1393\text{ cm}^{-1}$ ,  $1450\text{ cm}^{-1}$ , and  $1510\text{ cm}^{-1}$  peaks are related to the amines stretching ( $\nu_{\text{N-H}}$ ); the peak at  $3300\text{ cm}^{-1}$  could be related to the residual OH groups; the band at  $1611\text{ cm}^{-1}$  is related C=C of the aromatic ring and the band at  $2840\text{ cm}^{-1}$  is a characteristic of C–H-trenching vibrations.

### NMR analysis

The ER structure was confirmed by the  $^1\text{H}$  and  $^{31}\text{P}$ . NMR spectra are shown in Fig. 7. The epoxy resin  $^1\text{H}$  signals for ER (ppm, DMSO- $d_6$ ) were observed at 2.38–2.63 (dd, 2H,  $\text{CH}_2$ ) (A,B), 2.77 (m, 1H, CH oxirane) (X), 3.36–3.61 (dd, O- $\text{CH}_2$ ) (C,D), 4 (s, 1H, –NH secondary), and 6.71–7.11 (s, 4H aromatic). Furthermore,  $^{31}\text{P}$  NMR (ppm, DMSO- $d_6$ ) exhibits two peaks at 2.3 (s) correspond to P=O and 17.3 (s) correspond to N–P.

### Thermal analysis

Thermal analysis was carried out using DSC. The DSC is often used to characterize the polymers thermal transition from the glass transition temperature ( $T_g$ ) measurement. A simplistic view of a material's glass transition is the temperature below which molecules has low mobility, so polymers are rigid and brittle below their  $T_g$ .

The DSC' results corresponding to ER–MDA and ER–MDA–ZP are shown in Fig. 8.

The  $T_g$  values shown in the thermograms ranged from 100 and  $160\text{ }^\circ\text{C}$ . The MDA-cured ER epoxy system displayed a  $T_g$  value of about  $118.74\text{ }^\circ\text{C}$ . However, the  $T_g$  value increased to  $151.22\text{ }^\circ\text{C}$  in the presence of 5 wt% of

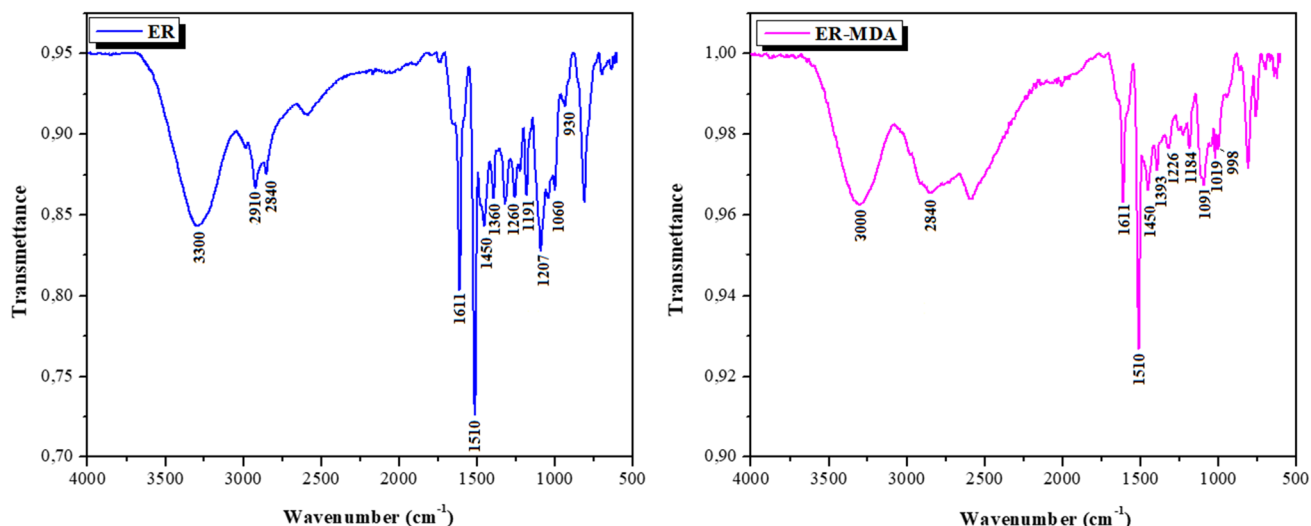


**Fig. 6** ATR-FTIR spectra of hexaglycidyl tris (*p*-ethylene dianiline) phosphoric triamide (ER) and of the epoxy resin cured with methylene dianiline (ER-MDA) on steel surface

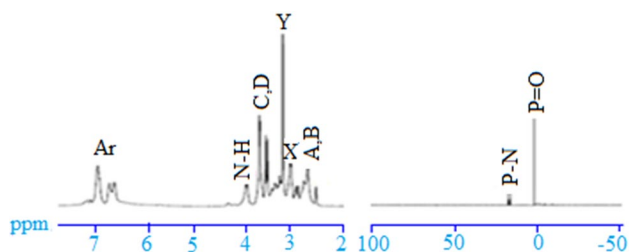


**Fig. 7** NMR spectra of hexaglycidyl tris (*p*-ethylene dianiline) phosphoric triamide (ER)

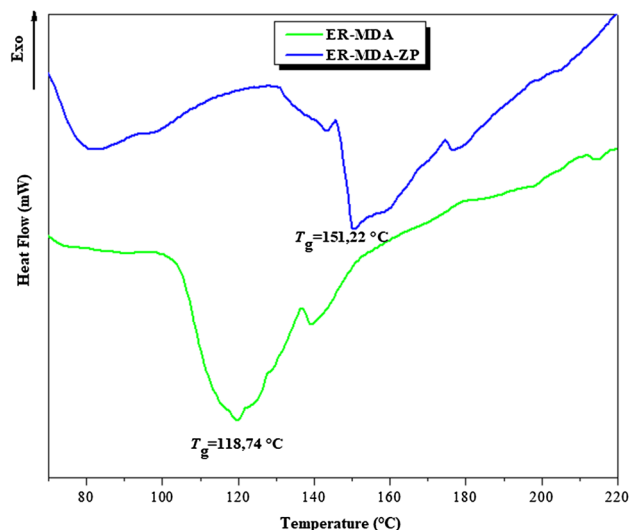


**Fig. 8** DSC curves of ER-MDA and ER-MDA-ZP tested materials

zinc phosphate, the increase in  $T_g$  could be attributed to the effect of the ZP particles on the polymer matrix, which would decrease polymer chain mobility by forming physical crosslinks between polymer chains and thus increases its thermal properties [24]. This is a very interesting result from an industrial point of view, because high  $T_g$  values are frequently requested to fulfill some of the main industrial requirements of structural materials in several fields (aeronautics, marine industry, etc.).

### Corrosion resistance of the coatings

The EIS is a proper approach for gaining an insight into the coatings corrosion resistance in the different corrosive environment [25, 26]. Therefore, it was used to study the behaviors of the carbon steel samples coated with epoxy at room temperature.

The coating resistance ( $R_{coat}$ ) and charge transfer resistance ( $R_{ct}$ ) of the coated carbon steel electrodes were obtained by fitting the equivalent circuit to the analysis data in a software.

The Bode plots of the epoxy coated steel samples are shown in Fig. 9, which obtained after 2000 h of exposure to UV and 1 h of immersion in 3 wt% NaCl. The evaluation was carried out by measuring the impedance modulus.

The impedance modulus at low frequency ( $Z_f=0.01$  Hz) is an important parameter to detect the anticorrosive protection properties of the coatings.

For the ER-MDA coating, the impedance modulus at  $Z_f=0.01$  Hz was  $1.744 \times 10^4 \Omega \text{ cm}^2$  after 1 h of immersion

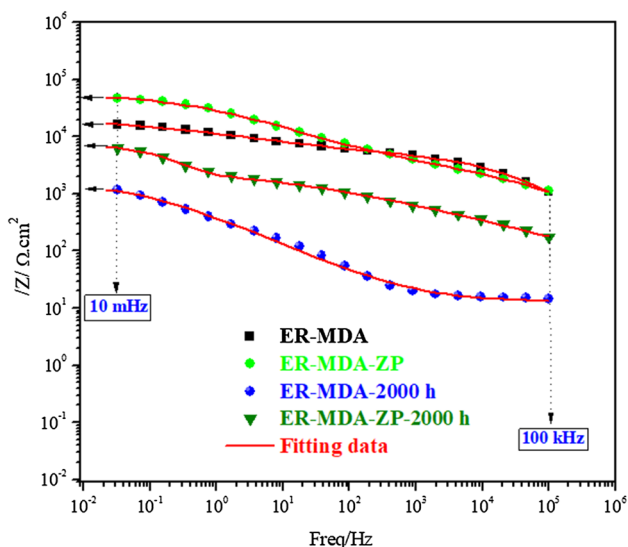


**Fig. 9** Bode plots of the ER-MDA and ER-MDA-ZP coatings after 2000 h of exposure to UV and 1 h of immersion in 3 wt% NaCl

in 3 wt% NaCl. However, the value dropped to  $1.262 \times 10^3 \Omega \text{ cm}^2$  after 2000 h of exposure to UV and 1 h of immersion in 3 wt% NaCl. The results indicate that the exposure to UV radiation causes the coating to deteriorate and losses its protective ability. In the case of the ER-MDA-ZP coating, the initial impedance modulus at  $Z_f = 0.01 \text{ Hz}$  was  $5.004 \times 10^4 \Omega \text{ cm}^2$  after 1 h of immersion in 3 wt% NaCl. The value dropped to  $6.946 \times 10^3 \Omega \text{ cm}^2$  after 2000 h of exposure to UV and 1 h of immersion in 3 wt% NaCl.

The results suggest that the ER-MDA-ZP coating provides an excellent corrosion resistance performance to carbon steel. Therefore, the presence of the zinc phosphate improved the performance of the epoxy coating by enhancing its stability and its barrier properties against the salts diffusion towards the metal/coating interface [27].

Quantitative analysis of the protective properties of the ER-MDA and ER-MDA-ZP coatings was performed by fitting the EIS curves with the equivalent electric circuit displayed in Fig. 10.

In the circuit, the electrolyte resistance ( $R_s$ ), coating resistance ( $R_{\text{coat}}$ ), and charge transfer resistance ( $R_{\text{ct}}$ ) of corrosion reaction on the steel substrate were calculated. In addition to the coating capacitance ( $C_{\text{coat}}$ ) and double-layer (steel/solution) capacitance ( $C_{\text{dl}}$ ) [28], the total resistance ( $R_t$ ) was calculated according to the values of charge transfer resistance and coating resistance ( $R_t = R_{\text{ct}} + R_{\text{coat}} - R_s$ ). The coating capacitance values ( $C_{\text{coat}}$  and  $C_{\text{dl}}$ ) are calculated using Eq. (1) [29]:

$$C_x = \frac{(R_x \text{CPE})^{\frac{1}{n}}}{R_x} \tag{1}$$

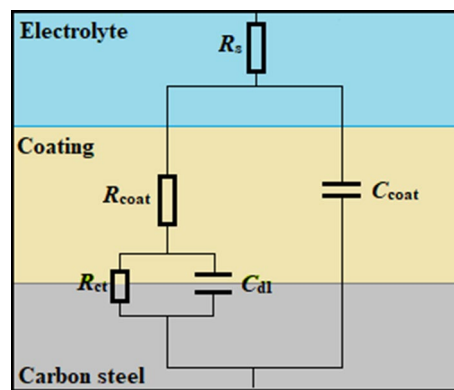


**Fig. 10** Equivalent electrical circuit to model the impedance spectra

where  $C$  represents the capacity, CPE is a nonideal capacity (commonly named constant phase element),  $R$  is resistance, and  $n$  is a capacity factor. The electrochemical parameters values are given in Table 3.

The Nyquist plots of the ER-MDA and ER-MDA-ZP coatings after 2000 h UV exposure and 1 h of immersion in 3 wt% NaCl are shown in Fig. 11.

The values of electrochemical impedance resulting from the epoxy coatings after 2000 h UV exposure and after 1 h of immersion in 3 wt% NaCl are summarized in Table 3.

The data presented in Fig. 12 are the total resistance ( $R_t$ ) for the two epoxy coatings after 2000 h UV exposure and 1 h of immersion in 3 wt% NaCl.

The notable effect on the performance of the ER-MDA coating is clearly observed. On the other hand, the ER-MDA-ZP coating provided a better corrosion protection efficiency for carbon steels.

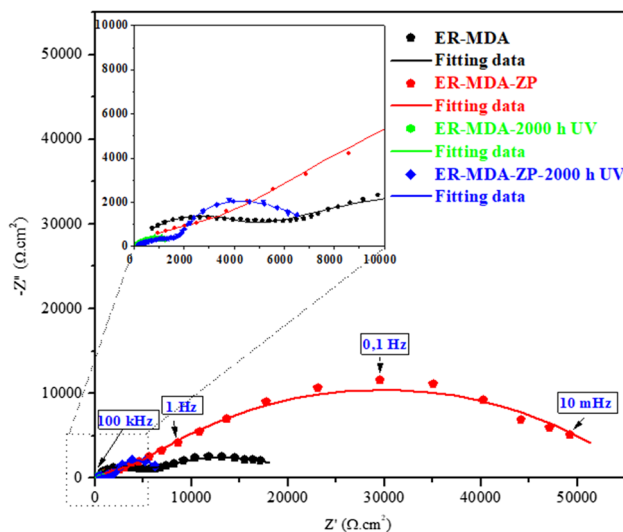
The diffusion of electrolytes into the ER-MDA coating, which is controlled by the crosslinking density and type of crosslinking functionalities (polar or nonpolar), could cause a decrease in the barrier efficiency. The drop in the efficiency usually starts with the formation of microholes and defects in the film, causing the coating to fail as a barrier. The ER-MDA-coating degradation after 2000 h of exposure to UV led to a drastic drop in the resistance of the coating. As a result of that, the corrosive agent was able to diffuse into the metal/coating interface, causing a sharp drop in the impedance of the coating. From the results, we could conclude that the existence of ZP facilitated the formation of a passivating phosphate layer between the steel substrates and the coating matrix, while the well-dispersed zinc phosphate acted as an excellent barrier that prevents the diffusion of electrolytes through the coating to steel surface [30].

### EIS characteristics of coatings after UV exposure

The EIS results approved the mechanism proposed for preventing the degradation of the coating under UV exposure

**Table 3** Different electrochemical parameters extracted from EIS measurements after 2000 h of exposure to UV and 1 h of immersion in 3 wt% NaCl

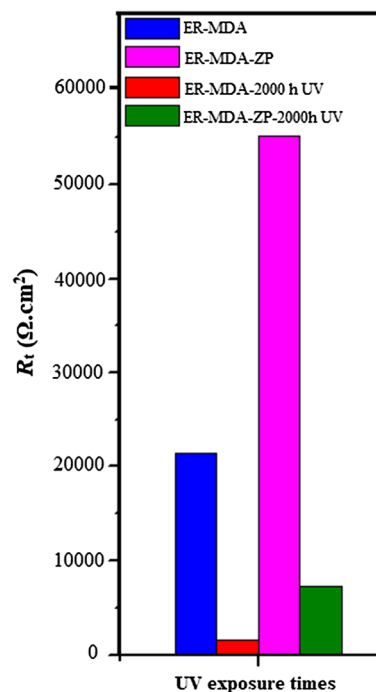
	$R_s$ ( $\Omega$ cm <sup>2</sup> )	$C_{\text{coat}}$ ( $\mu\text{F cm}^{-2}$ )	$R_{\text{coat}}$ ( $\Omega$ cm <sup>2</sup> )	$C_{\text{dl}}$ ( $\mu\text{F cm}^{-2}$ )	$R_{\text{ct}}$ ( $\Omega$ cm <sup>2</sup> )	$R_t$ ( $\Omega$ cm <sup>2</sup> )
ER-MDA	168	0.18	4342	42.39	17,209	21,383
ER-MDA-ZP	127	11.09	21,494	0.57	44,968	55,143
ER-MDA-2000 h	16.6	41.61	173	0.72	1468	1621
ER-MDA-ZP-2000 h	50.8	74.39	2408	0.29	4865	7264

**Fig. 11** Nyquist plots of the (ER-MDA and ER-MDA-ZP) coatings after 2000 h of exposure to UV and 1 h of immersion in 3 wt% NaCl

for two the matrices of ER-MDA and ER-MDA-ZP coatings (Fig. 13).

By increasing the exposure time up to 2000 h, some variations were observed in the resistances of the ER-MDA and ER-MDA-ZP coatings, showing that the rate of degradation by UV radiation was increased and the resistance of both coatings decreased by 7 and 13 times, respectively, after 2000 h of exposure to UV and 1 h of immersion in 3 wt% NaCl, as shown in Figs. 9 and 11.

After 2000 h of exposure to UV and the samples are submerged in the corrosive media, microcracks developed in the coating that allowed the electrolyte to diffuse towards the interface of metal/coating. Penetration of the electrolyte led to decreasing of the ER-MDA-coating impedance. With increasing immersion time, the microcracks were filled with the 3 wt% NaCl solution. After 1 h of immersion, the corrosion products, such as rust, fill microcracks temporarily. However, probably due to the presence of the ZP in its matrix, the ER-MDA-ZP coating showed a limited degradation. ZP seems to prevent the propagation of the microcracks, thus preventing the electrolytes from reaching the metal/coating interface. In

**Fig. 12** Variation of  $R_t$  for the (ER-MDA and ER-MDA-ZP) coatings after 2000 h of exposure to UV and 1 h of immersion in 3 wt% NaCl

addition, it could be that the ZP adds to the coating self-repair properties.

For this reason, the impedance of the ER-MDA-ZP coating after 2000 h UV exposure and 1 h immersion in corrosive media was higher than that for ER-MDA coating.

## Conclusions

In this study, the suitability of epoxy resin as an anticorrosive protection material for steel was evaluated. Two coating formulations were prepared, applied onto steel, and evaluated. The epoxy used for this purpose was hexaglycidyl tris (*p*-ethylene dianiline) phosphoric triamide (ER), it was synthesized at the laboratory, and its structural characterization was carried out by FTIR and NMR (<sup>1</sup>H and <sup>31</sup>P). The first



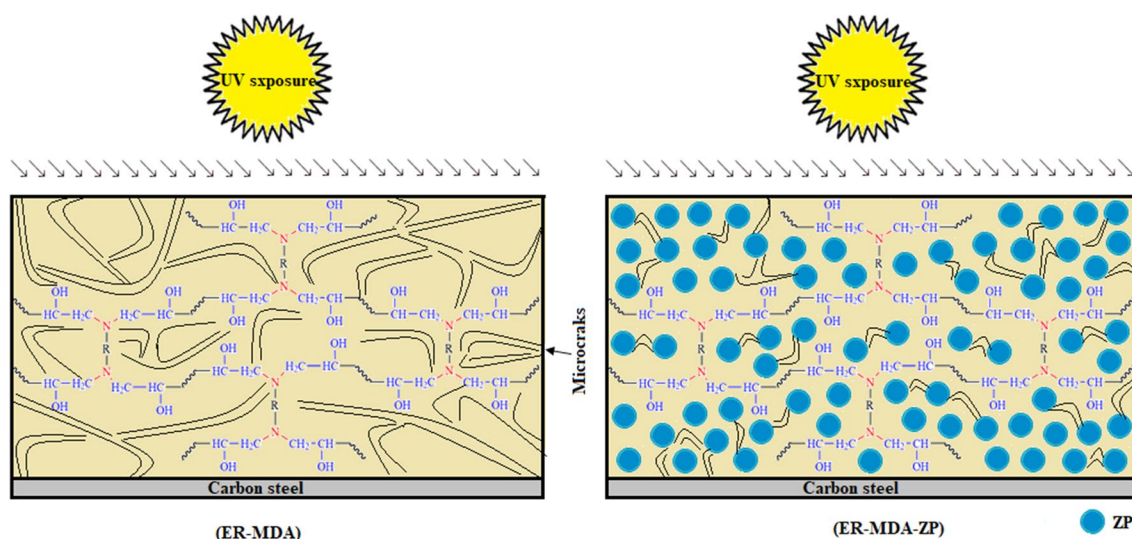


**Fig. 13** Schematic illustration of the mechanism of zinc phosphate to avoid the deterioration of the two epoxy coatings exposed to the action of UV rays

formulation (ER–MDA) composed of cured epoxy resin, while the second one (ER–MDA–ZP) contains zinc phosphate (5 wt%) additive besides epoxy resin. Nontoxic solvent isopropyl alcohol was used in the preparing the coating formulas. DSC analysis results showed that (ER–MDA–ZP) formula has higher glass transition temperature (151.22 °C) than the formulation (ER–MDA) (118.74 °C). Samples of steels coated with both formulas were evaluated in a NaCl (3 wt%) solution; accelerated weather testing was performed by exposure to UV. The protection efficiency of standard epoxy coating decreased after 2000 h of exposure to UV. However, the epoxy coating-containing ZP showed a much lower rate of degradation after exposure to UV, which could be related to the presence of zinc phosphate. The presence of ZP enhanced the protective effect of the coating and reduced the corrosive effect of the medium on the carbon steel. The results were proved by EIS study.

**Open Access** This article is distributed under the terms of the Creative Commons Attribution 4.0 International License (<http://creativecommons.org/licenses/by/4.0/>), which permits unrestricted use, distribution, and reproduction in any medium, provided you give appropriate credit to the original author(s) and the source, provide a link to the Creative Commons license, and indicate if changes were made.

## References

- Luciano G, Brinkmann A, Mahanty S, Echeverría M (2017) Development and evaluation of an eco-friendly hybrid epoxy-silicon coating for the corrosion protection of aluminium alloys. *Prog Org Coat* 110:78–85
- Pourhashem S, Vaezi MR, Rashidi A, Bagherzadeh MR (2017) Exploring corrosion protection properties of solvent based epoxy-graphene oxide nanocomposite coatings on mild steel. *Corros Sci* 115:78–92
- Mahidashti Z, Ramezanzadeh B, Bahlakeh G (2018) Screening the effect of chemical treatment of steel substrate by a composite cerium-lanthanum nanofilm on the adhesion and corrosion protection properties of a polyamide-cured epoxy coating; experimental and molecular dynamic simulations. *Prog Org Coat* 114:188–200
- Xiong Y, Jiang Z, Xie Y, Zhang X, Xu W (2013) Development of a DOPO-containing melamine epoxy hardeners and its thermal and flame-retardant properties of cured products. *J Appl Polym Sci* 127(6):4352–4358
- Naderi R, Attar M (2008) Electrochemical assessing corrosion inhibiting effects of zinc aluminum polyphosphate (ZAPP) as a modified zinc phosphate pigment. *Electrochim Acta* 53(18):5692–5696
- Carboneras M, Hernández L, Del Valle J, García-Alonso M, Escudero M (2010) Corrosion protection of different environmentally friendly coatings on powder metallurgy magnesium. *J Alloy Compd* 496(1–2):442–448
- Naderi R, Attar M (2009) Electrochemical study of protective behavior of organic coating pigmented with zinc aluminum polyphosphate as a modified zinc phosphate at different pigment volume concentrations. *Prog Org Coat* 66(3):314–320
- Shi C, Shao Y, Wang Y, Meng G, Liu B (2018) Influence of sub-micron-sheet zinc phosphate synthesised by sol–gel method on anticorrosion of epoxy coating. *Prog Org Coat* 117:102–117
- Hao Y, Liu F, Han E-H, Anjum S, Xu G (2013) The mechanism of inhibition by zinc phosphate in an epoxy coating. *Corros Sci* 69:77–86
- Zhang W, Li X, Yang R (2011) Pyrolysis and fire behaviour of epoxy resin composites based on a phosphorus-containing poly-hedral oligomeric silsesquioxane (DOPO-POSS). *Polym Degrad Stab* 96(10):1821–1832
- Dagdag O, El Harfi A, Essamri A, El Bachiri A, Hajjaji N, Erramli H, Hamed O, Jodeh S (2018) Anticorrosive performance of new epoxy-amine coatings based on zinc phosphate tetrahydrate as a nontoxic pigment for carbon steel in NaCl medium. *Arab J Sci Eng*. <https://doi.org/10.1007/s13369-018-3160-z>
- Dagdag O, El Harfi A, El Gouri M, Touhami ME, Essamri A, Cherkaoui O (2016) Electrochemical impedance spectroscopy



- (SIE) evaluation of the effect of immersion time of the protective matrix based on a polymer tetra glycidyl of ethylene dianiline (TGEDA) on carbon steel in 3% NaCl. *Int J ChemTech Res* 9(04):390–399
13. El Gouri M, El Bachiri A, Hegazi SE, Rafik M, El Harfi A (2009) Thermal degradation of a reactive flame retardant based on cyclotriphosphazene and its blend with DGEBA epoxy resin. *Polym Degrad Stab* 94(11):2101–2106
  14. Huo S, Wang J, Yang S, Zhang B, Chen X, Wu Q, Yang L (2017) Synthesis of a novel reactive flame retardant containing phosphaphenanthrene and piperidine groups and its application in epoxy resin. *Polym Degrad Stab* 146:250–259
  15. Ferdosian F, Ebrahimi M, Jannesari A (2013) Curing kinetics of solid epoxy/DDM/nanoclay: isoconversional models versus fitting model. *Thermochim Acta* 568:67–73
  16. Jin F-L, Li X, Park S-J (2015) Synthesis and application of epoxy resins: a review. *J Ind Eng Chem* 29:1–11
  17. Shao Y, Jia C, Meng G, Zhang T, Wang F (2009) The role of a zinc phosphate pigment in the corrosion of scratched epoxy-coated steel. *Corros Sci* 51(2):371–379
  18. Liu Z, Zhang G, Liu Z, Sun H, Zhao C, Wang S, Li G, Na H (2012) Synthesis and properties of an epoxy resin containing trifluoromethyl side chains and its cross-linking networks with different curing agents. *Polym Degrad Stab* 97(5):691–697
  19. Liu R, Wang X (2009) Synthesis, characterization, thermal properties and flame retardancy of a novel nonflammable phosphazene-based epoxy resin. *Polym Degrad Stab* 94(4):617–624
  20. Wang C-S, Shieh J-Y (2000) Synthesis and properties of epoxy resins containing bis (3-hydroxyphenyl) phenyl phosphate. *Eur Polym J* 36(3):443–452
  21. Gu L, Chen G, Yao Y (2014) Two novel phosphorus–nitrogen-containing halogen-free flame retardants of high performance for epoxy resin. *Polym Degrad Stab* 108:68–75
  22. Delor-Jestin F, Drouin D, Cheval P-Y, Lacoste J (2006) Thermal and photochemical ageing of epoxy resin—influence of curing agents. *Polym Degrad Stab* 91(6):1247–1255
  23. Kocaman S, Ahmetli G (2016) A study of coating properties of biobased modified epoxy resin with different hardeners. *Prog Org Coat* 97:53–64
  24. Zhao DL, Li X, Shen ZM (2008) Microwave absorbing property and complex permittivity and permeability of epoxy composites containing Ni-coated and Ag filled carbon nanotubes. *Compos Sci Technol* 68(14):2902–2908
  25. Collazo A, Nóvoa X, Pérez C, Puga B (2010) The corrosion protection mechanism of rust converters: an electrochemical impedance spectroscopy study. *Electrochim Acta* 55(21):6156–6162
  26. Sakhri A, Perrin F, Aragon E, Lamouric S, Benaboura A (2010) Chlorinated rubber paints for corrosion prevention of mild steel: a comparison between zinc phosphate and polyaniline pigments. *Corros Sci* 52(3):901–909
  27. Avci G (2008) Corrosion inhibition of indole-3-acetic acid on mild steel in 0.5 M HCl. *Colloids Surf A* 317(1–3):730–736
  28. Guo B, Finne-Wistrand A, Albertsson A-C (2010) Molecular architecture of electroactive and biodegradable copolymers composed of polylactide and carboxyl-capped aniline trimer. *Biomacromol* 11(4):855–863
  29. Yu D, Wen S, Yang J, Wang J, Chen Y, Luo J, Wu Y (2017) RGO modified ZnAl-LDH as epoxy nanostructure filler: a novel synthetic approach to anticorrosive waterborne coating. *Surf Coat Technol* 326:207–215
  30. Ramezanzadeh B, Attar M (2011) Studying the corrosion resistance and hydrolytic degradation of an epoxy coating containing ZnO nanoparticles. *Mater Chem Phys* 130(3):1208–1219

**Publisher's Note** Springer Nature remains neutral with regard to jurisdictional claims in published maps and institutional affiliations.

